Theoretical Evaluation of Steric Effects in $[ReH_5(PR_3)_2(SiR_3)_2]$ Complexes with the IMOMM Method

Guada Barea,[†] Feliu Maseras,*[,†,‡] Yves Jean,[§] and Agustí Lledós[†]

Unitat de Química Física, Departament de Química, Universitat Autònoma de Barcelona, 08193 Bellaterra, Barcelona, Catalonia, Spain, Laboratoire de Structure et Dynamique des Systèmes Moléculaires et Solides, UMR 5636, Université de Montpellier II, 34095 Montpellier Cedex 5, France, and Laboratoire de Chimie Théorique (CNRS URA 506, ICMO), Bat. 490, Université de Paris-Sud, 91405 Orsay Cedex, France

Received April 24, 1996[⊗]

A theoretical study including full geometry optimizations is carried out at the IMOMM(MP2:MM3) (IMOMM = integrated molecular orbital molecular mechanics) computational level on the $[ReH_5(PPh^iPr_2)_2(SiHPh_2)_2]$ and $[ReH_5(PCyp_3)_2(SiH_2Ph)_2]$ systems, the results being compared with available experimental diffraction data, as well as with MP2 results on the model system $[ReH_5(PH_3)_2(SiH_3)_2]$. A simple scheme for the analysis of the relative weight of different contributions to the "steric" distortion is also proposed and applied to the same $[ReH_5(PPh^iPr_2)_2(SiHPh_2)_2]$ and $[ReH_5(PCyp_3)_2(SiH_2Ph)_2]$ species.

Introduction

The recently proposed "integrated molecular orbital molecular mechanics" (IMOMM) computational scheme aims to overcome the traditional division of theoretical calculations on transition metal complexes between MO-based calculations on model systems and MM-based calculations on real systems through integration of both computational approaches in the same calculation.[1] Both separate approaches have yielded satisfactory results in a number of cases, their abilities being complementary: MO-based calculations are strong in the description of the number and nature of metal−ligand bonds,[2] while MM-based calculations are strong in describing the long-range ligand−ligand interactions.[3] These two different types of interaction will be referred to as "electronic" and "steric" throughout this paper.

Some calibration tests of IMOMM have already been published, most of them based on comparison with much more expensive ab initio calculations on the complete systems, and production calculations on the chemical properties of a variety of systems are currently under way.[4] This paper provides yet another test of IMOMM, but from a slightly different point of view. Here, quality of the results will be assessed from comparison between optimized IMOMM structures and crystal structures. In particular, two nine-coordinate species of the $[ReH_5(PR_3)_2(SiR_3)_2]$ stoichiometry will be analyzed,[5] with special attention to the eventual improvement introduced by the IMOMM correction on the qualitatively correct results obtained on ab initio calculations on the model system $[ReH_5(PH_3)_2(SiH_3)_2]$.

A second goal of this paper is the exploitation of the capabilities of IMOMM for the analysis of the results. Electronic and steric effects can be quantitatively separated, and the steric part can be fully decomposed. The possibilities and limitations of this analysis will be discussed in some detail.

Computational Details

IMOMM calculations are performed with a program built from modified versions of two standard programs: Gaussian 92/DFT[6] for the quantum mechanics part and mm3(92)[7] for the molecular mechanics part. Ab initio calculations are carried out on the $[ReH_5(PH_3)_2(SiH_3)_2]$ fragment at the MP2 level with consideration of excitations concerning the outermost 42 electrons (frozen core approach).[8] A quasirelativistic effective core potential replaces the 60 electron core of the Re atom,[9] as well as the 10 electron core of the P and Si atoms.[10] The basis set for Re is that associated to the pseudopotential[9] with the standard valence double-ζ LANL2DZ contraction.[6] The basis set for P and Si is also that associated to the corresponding pseudopotentials (LANL1DZ),[10] supplemented in this case by a polarization d shell.[11] The basis set for the hydrogen atoms is double-ζ,,[12] supplemented with a polarization p shell in the case of hydrogen atoms directly attached to the metal atom.[13]

Polarization functions are therefore added on all the atoms directly attached to the rhenium atom. They are not added on the rhenium atom itself because they should be of f type, and Gaussian 92/DFT does not provide analytic gradients for this type of orbitals. At any rate, we tested the effect f orbitals[14] had on the geometry optimization

† Universitat Autònoma de Barcelona.
‡ Université de Montpellier II.
§ Université de Paris-Sud.
⊗ Abstract published in *Advance ACS Abstracts,* September 15, 1996.

(1) Maseras, F.; Morokuma, K. *J. Comput. Chem.* **1995**, *16*, 1170.
(2) (a) Veillard, A. *Chem. Rev.* **1991**, *91*, 743. (b) Koga, N.; Morokuma, K. *Chem. Rev.* **1991**, *91*, 823.
(3) (a) Comba, P.; Hambley, T. W. *Molecular Modeling of Inorganic Compounds*; VCH: Weinheim, Germany, 1995. (b) Zimmer, M. *Chem. Rev.* **1995**, *95*, 2629.
(4) (a) Matsubara, T.; Maseras, F.; Koga, N.; Morokuma, K. *J. Phys. Chem.* **1996**, *100*, 2573. (b) Ujaque, G.; Maseras, F.; Lledós, A. *Theor. Chim. Acta*, in press.
(5) Howard, J. A. K.; Keller, P. A.; Vogt, T.; Taylor, A. L.; Dix, N. D.; Spencer, J. L. *Acta Crystallogr.* **1992**, *B48*, 438.
(6) Frisch, M. J.; Trucks, G. W.; Schlegel, H. B.; Gill, P. M. W.; Johnson, B. G.; Wong, M. W.; Foresman, J. B.; Robb, M. A.; Head-Gordon, M.; Replogle, E. S.; Gomperts, R.; Andres, J. L.; Raghavachari, K.; Binkley, J. S.; Gonzalez, C.; Martin, R. L.; Fox, D. J.; Defrees, D. J.; Baker, J.; Stewart, J. J. P.; Pople, J. A. *Gaussian 92/DFT*; Gaussian, Inc.: Pittsburgh, PA, 1993.
(7) Allinger, N. L. *MM3(92)*; Quantum Chemistry Program Exchange: Bloomington, IN, 1992.
(8) Møller, C.; Plesset. M. S. *Phys. Rev.* **1934**, *46*, 618.
(9) Hay, P. J.; Wadt, W. R. *J. Chem. Phys.* **1985**, *82*, 299.
(10) Wadt, W. R.; Hay, P. J. *J. Chem. Phys.* **1985**, *82*, 284.
(11) Francl, M. M.; Pietro, W. J.; Hehre, W. J.; Binkley, J. S.; Gordon, M. S.; DeFrees, D. J.; Pople, J. A. *J. Chem. Phys.* **1982**, *77*, 3654.
(12) Hehre, W. J.; Ditchfield, R.; Pople, J. A. *J. Chem. Phys.* **1972**, *56*, 2257.
(13) Hariharan, P. C.; Pople, J. A. *Theor. Chim. Acta* **1973**, *28*, 213.
(14) Ehlers, A. W.; Böhme, M.; Dapprich, S.; Gobbi, A.; Höllwarth, A.; Jonas, V.; Köhler, K. F.; Stegmann; Veldkamp, A.; Frenking, G. *Chem. Phys. Lett.* **1993**, *208*, 111.

S0020-1669(96)00440-5 CCC: $12.00

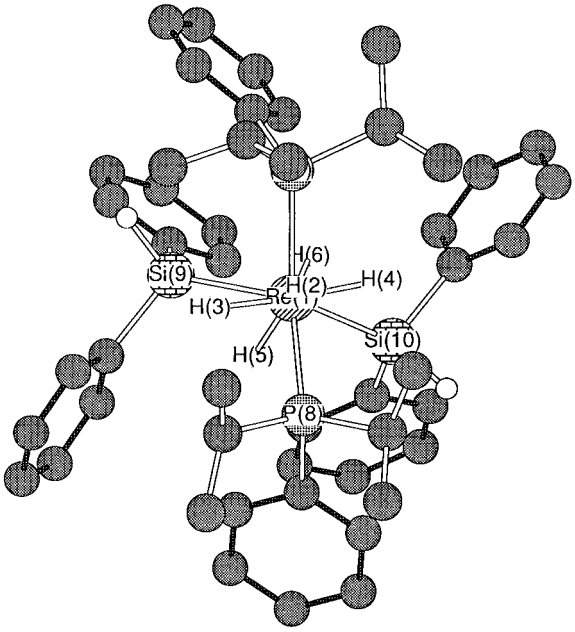

Figure 1. Experimental structure of the $[ReH_5(PPh^iPr_2)_2(SiHPh_2)_2]$ complex (**1**), as taken from neutron diffraction data.[5,18] Hydrogen atoms not directly attached to the metal are omitted for simplicity.

of $[ReH_9]^{2-}$,[15] and we found it to be quite small. The optimized values for the two non-equivalent Re−H distances of this D_{3h} anion are 1.702 and 1.665 Å without f orbitals and 1.689 and 1.650 Å when they are included. Differences are in the range of 0.01 Å, rendering unnecessary the large computational effort required for introduction of the f polarization shell. It is also worth mentioning that the optimized geometry for $[ReH_9]^{2-}$ with our computational method is close to that presented by previous experimental[14] and theoretical[16] reports.

Molecular mechanics calculations on the full system use the mm3-(92) force field.[7] Van der Waals parameters for the rhenium atom are taken from the UFF force field,[17] and torsional contributions involving dihedral angles with the metal atom in terminal position are set to zero. Geometry optimizations are full except for the P−H (1.42 Å) and Si−H (1.49 Å) bond distances in the MO part of IMOMM and the $P-C_{sp^3}$ (1.843 Å), $P-C_{sp^2}$ (1.828 Å), and Si−C (1.856 Å) distances in the MM part of IMOMM.

In what follows IMOMM(MP2:MM3) will refer to IMOMM calculations where the quantum mechanics calculation is performed on the $[ReH_5(PH_3)_2(SiH_3)_2]$ system at the MP2 level with the basis set indicated above and the molecular mechanics calculation is carried out on the full system with the MM3 force field containing the modifications just mentioned.

Experimental Data on the $[ReH_5(PR_3)_2(SiR_3)_2]$ Systems

The crystallographic characterization of two different complexes of the $[ReH_5(PR_3)_2(SiR_3)_2]$ type containing exclusively monodentate ligands can be found in the literature.[5] They are $[ReH_5(PPh^iPr_2)_2(SiHPh_2)_2]$ (**1**) and $[ReH_5(PCyp_3)_2(SiH_2Ph)_2]$ (**2**). Their crystal structures are presented in Figures 1 and 2, respectively, with experimental bond distances and bond angles contained in Tables 1−3, together with the computed values. Neutron diffraction data are available for **1**, while only X-ray diffraction results are available for **2**. This poses a serious limitation in the precision of all geometrical parameters involving hydrogen atoms in the case of **2**. However, similarities between the two species are quite obvious, and there is no reason to expect serious differences in their coordination polyhedron.

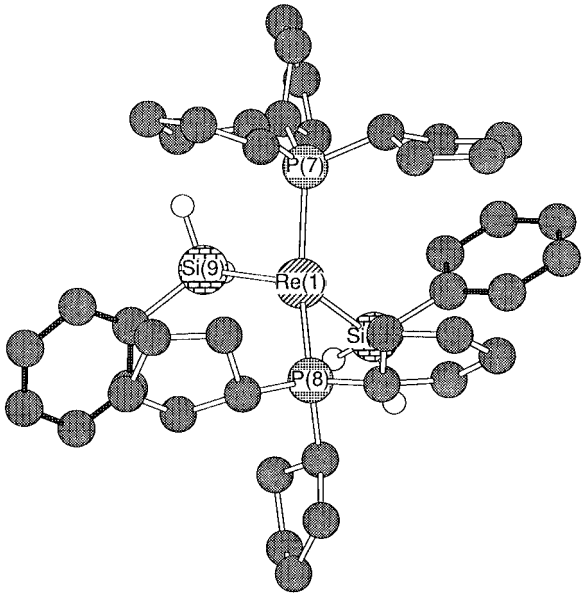

Figure 2. Experimental structure of the $[ReH_5(PCyp_3)_2(SiH_2Ph)_2]$ complex (**2**), as taken from X-ray diffraction data.[5,18] Hydrogen atoms not directly attached to the metal are omitted for simplicity.

Table 1. Metal−Ligand Bond Distances (Å) for the Different Complexes $[ReH_5(PPh^iPr_2)_2(SiHPh_2)_2]$ (**1**), $[ReH_5(PCyp_3)_2(SiH_2Ph)_2]$ (**2**), and $[ReH_5(PH_3)_2(SiH_3)_2]$ (**3**): Computed Values at the IMOMM(MP2:MM3) and MP2 Levels, as Well as Experimental Values

	1 (expt)	**2** (expt)	**3** (MP2)	**1** (IMOMM)	**2** (IMOMM)
Re(1)−H(2)	1.698		1.692	1.689	1.685
Re(1)−H(3)	1.704		1.698	1.691	1.691
Re(1)−H(4)	1.707		1.698	1.690	1.679
Re(1)−H(5)	1.676		1.688	1.676	1.679
Re(1)−H(6)	1.684		1.688	1.676	1.679
Re(1)−P(7)	2.444	2.439	2.402	2.467	2.465
Re(1)−P(8)	2.444	2.444	2.402	2.466	2.466
Re(1)−Si(9)	2.510	2.490	2.560	2.566	2.554
Re(1)−Si(10)	2.500	2.510	2.560	2.567	2.553

Both complexes **1** and **2** correspond to the same coordination polyhedron, a capped square antiprism, a quite common polyhedron for nine-coordinate species.[19] The capping position is occupied by one hydride ligand, labeled as H(2), with the two phosphine ligands and two hydride ligands (H(3) and H(4)) in the capped face and the two silyl ligands and the other two hydride ligands H(5) and H(6) in the noncapped square face. The overall capped square antiprism geometry is quite clear, with two well-differentiated sets of L−M−L angles with respect to the capping ligand (72.1, 73.3, 70.1, and 71.1° on one hand; 139.2, 140.2, 119.7, and 122.4° on the other hand for complex **1**). No direct interactions are observed between the hydride ligands, the shortest H−H distance in **1** being 2.003 Å for H(2)−H(4). Both geometries of **1** and **2** are slight distortions from the C_2 symmetry, with the symmetry axis containing Re(1) and H(2), the distortion being likely associated with packing effects.

Despite the qualitative similarities, there are some quantitative differences between the two species, especially in what concerns the bond angles. The largest discrepancy is in Si(9)−Re(1)−Si(10), that is, 117.9° in **1** and 97.9° in **2** (Table 1). Testing the ability of the IMOMM scheme to reproduce these differences is one of the goals of the present work. Another goal is checking its intrinsic accuracy for the two different complexes. Finally,

(15) Abrahams, S. C.; Ginsberg, A. P.; Knox, K. *Inorg. Chem.* **1964**, *4*, 558.
(16) Shen, M.; Schaefer, Henry, F., III; Partridge, H. *Mol. Phys.* **1992**, *76*, 995.
(17) Rappé, A. K.; Casewit, C. J.; Colwell, K. S.; Goddard, W. A., III; Skiff, W. M. *J. Am. Chem. Soc.* **1992**, *114*, 10024.
(18) Allen, F. H.; Davies, J. E.; Galloy, J. J.; Johnson, O.; Kennard, O.; Macrae, C. F.; Mitchell, E. M.; Mitchell, G. F.; Smith, J. M.; Watson, D. G. *J. Chem. Inf. Comput. Sci.* **1991**, *31*, 187.
(19) Guggenberger, L. J.; Muetterties, E. L. *J. Am. Chem. Soc.* **1976**, *98*, 7221.

Table 2. Ligand−Metal−Ligand Bond Angles (deg) Not Involving Hydrogen Atoms for the Different Complexes $[ReH_5(PPh^iPr_2)_2(SiHPh_2)_2]$ (**1**), $[ReH_5(PCyp_3)_2(SiH_2Ph)_2]$ (**2**), and $[ReH_5(PH_3)_2(SiH_3)_2]$ (**3**): Computed Values at the IMOMM(MP2:MM3) and MP2 Levels, as Well as Experimental Values[a]

	1 (expt)	**2** (expt)	**3** (MP2)	**1** (IMOMM)	**2** (IMOMM)
P(7)−Re(1)−P(8)	142.2	139.5	143.2	143.5	140.3
P(7)−Re(1)−Si(9)	85.3	88.5	80.7	81.4	88.4
P(7)−Re(1)−Si(10)	115.2	118.8	124.3	119.5	117.1
Si(9)−Re(1)−Si(10)	117.9	97.9	100.8	113.8	102.1

[a] The overall C_2 symmetry is taken into account to avoid inclusion of redundant values.

Table 3. Ligand−Metal−Ligand Bond Angles (deg) Involving Hydrogen Atoms for the Complexes $[ReH_5(PPh^iPr_2)_2(SiHPh_2)_2]$ (**1**) and $[ReH_5(PH_3)_2(SiH_3)_2]$ (**3**): Computed Values at the IMMOM(MP2:MM3) and MP2 Levels, as Well as Experimental Values[a]

	1 (expt)	**3** (MP2)	**1** (IMOMM)
H(2)−Re(1)−H(3)	72.1	69.7	71.9
H(2)−Re(1)−H(5)	139.7	136.2	138.0
H(2)−Re(1)−P(7)	70.6	71.6	71.7
H(2)−Re(1)−Si(9)	121.1	129.6	123.1
H(3)−Re(1)−H(4)	145.4	139.5	142.0
H(3)−Re(1)−H(5)	128.2	137.4	134.3
H(3)−Re(1)−H(6)	80.6	76.3	77.6
H(3)−Re(1)−P(7)	91.5	87.4	90.9
H(3)−Re(1)−P(8)	77.1	80.0	77.3
H(3)−Re(1)−Si(9)	54.6	67.6	60.1
H(3)−Re(1)−Si(10)	152.6	145.2	148.7
H(5)−Re(1)−H(6)	80.7	87.6	84.2
H(5)−Re(1)−P(7)	140.8	134.2	136.9
H(5)−Re(1)−P(8)	74.5	76.0	74.6
H(5)−Re(1)−Si(9)	58.8	53.5	56.8
H(5)−Re(1)−Si(10)	74.4	71.1	74.8

[a] The overall C_2 symmetry is taken into account to avoid inclusion of redundant values.

these systems have been chosen also because of their close relationship to $[ReH_5(disil)(PPh_3)_2]$, involving a bidentate 1,2-bis(dimethylsilyl)benzene ligand and apparently containing an elongated dihydrogen ligand.[20] Understanding of bonding in these species can help give a better understanding of the nature of dihydrogen species.[21]

Geometry Optimization at the IMOMM Level

Full geometry optimizations are carried out at the IMOMM-(MP2:MM3) computational level for complexes **1** and **2**. These are compared to the experimental geometries of **1** and **2** and to the geometry of model complex $[ReH_5(PH_3)_2(SiH_3)_2]$ (**3**) optimized at the MP2 level. Selected parameters of these geometry optimizations are collected in Tables 1−3, with optimized geometries presented in Figures 3−5. The results for the metal−ligand bond distances presented in Table 1 show only a marginal improvement associated with the use of IMOMM. The Re−P distances that are underestimated by 0.04 Å in the MO calculation of **3** are overestimated by 0.02 Å in the IMOMM calculations of **1** and **2**. Re−Si distances are overestimated by *ca.* 0.06 Å in all cases, with a difference of *ca.* 0.01 Å between complexes **1** and **2** being properly reproduced by IMOMM. Re−H distances appear to be well-reproduced in all cases. All computed geometries have a C_2 symmetry, although no a priori restriction was introduced in the geometry optimization process.

Differences are much more significative in the case of the bond angles that, after all, are supposed to be more sensitive to the steric effects. Table 2 is a collection of results concerning

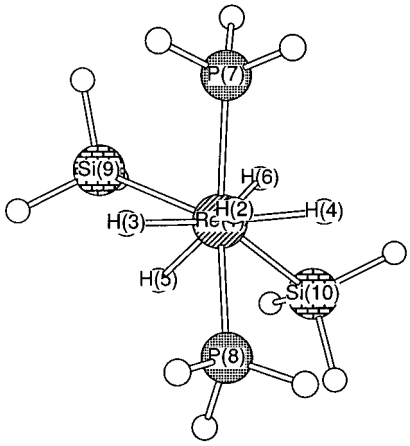

Figure 3. Optimized structure of the model complex $ReH_5(PH_3)_2(SiH_3)_2$ (**3**) at the MP2 computational level. Hydrogen atoms not directly attached to the metal are omitted for simplicity.

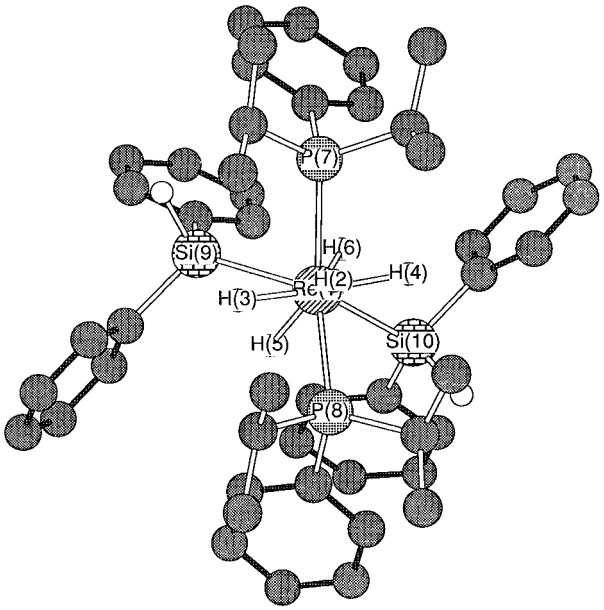

Figure 4. Optimized structure of the $[ReH_5(PPh^iPr_2)_2(SiHPh_2)_2]$ complex (**1**) at the IMOMM(MP2:MM3) computational level. Hydrogen atoms not directly attached to the metal are omitted for simplicity.

L−M−L bond angles involving the heavy P and Si atoms. These are the only bond angles available from the X-ray study of **2**. Reproduction of experimental values is substantially improved when going from the MP2 calculation on **3** to the IMOMM-(MP2:MM3) calculations on the real systems. For complex **1** the average deviation of the MP2 calculation is 8.0°, while that of the IMOMM calculation is 3.4°. Things are even better for **2**, where the average MP2 deviation of 4.7° drops to 1.7° at the IMOMM level. Even better, the difference between **1** and **2** is reproduced by the IMOMM calculation. Si(9)−Re−Si(10), experimentally larger by 20.0° in **1** than in **2**, is found by IMOMM to be 12.7° larger in **1** than in **2**.

These positive conclusions for IMOMM are confirmed when the L−M−L bond angles involving hydrogen atoms (Table 3)

(20) Loza, M. L.; De Gala, S. R.; Crabtree, R. H. *Inorg. Chem.* **1994**, *33*, 5073.
(21) (a) Kubas, G. J. *Acc. Chem. Res.* **1988**, *21*, 120. (b) Jessop, P. J.; Morris, R. H. *Coord. Chem. Rev.* **1992**, *121*, 155. (c) Crabtree, R. H. *Angew. Chem., Int. Ed. Engl.* **1993**, *32*, 789.

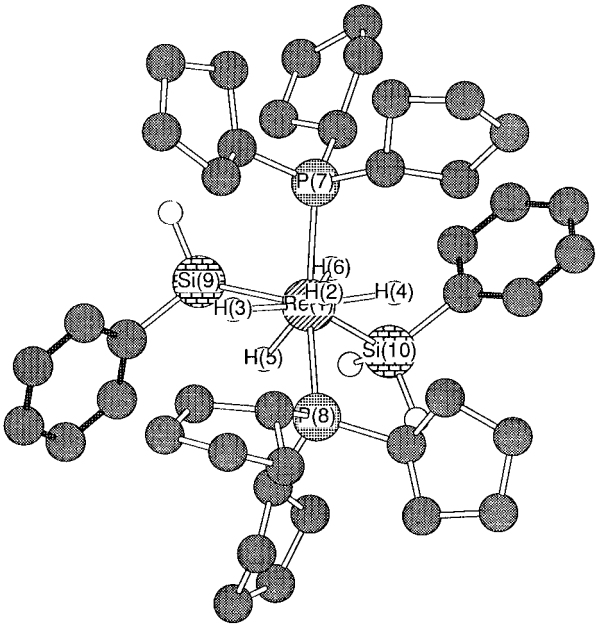

Figure 5. Optimized structure of the $[ReH_5(PCyp_3)_2(SiH_2Ph)_2]$ complex (**2**) at the IMOMM(MP2:MM3) computational level. Hydrogen atoms not directly attached to the metal are omitted for simplicity.

are included in the discussion. Although experimental values for these are only available from the neutron diffraction study of **1**, the larger number of parameters for this complex (up to 20 bond angles) gives more statistical significance to the results. The average difference between experimental bond angles for **1** and MP2 computed values for the model system **3** is 5.9° (Tables 2 and 3). In contrast the average difference between experimental and IMOMM(MP2:MM3) computed values for this same complex **1** is 2.7°. According to standard statistical criteria of accuracy, it can be concluded that IMOMM is significantly more precise than MP2.

Results presented in this section show consistently that IMOMM improves significantly the accuracy of the geometry optimization of species $[ReH_5(PPh^iPr_2)_2(SiHPh_2)_2]$ and $[ReH_5(PCyp_3)_2(SiH_2Ph)_2]$ with respect to the results obtained in the MP2 geometry optimization of $[ReH_5(PH_3)_2(SiH_3)_2]$. This is so despite the fact that the MP2 calculation already gave a qualitatively accurate result. Because of that, it should be expected that the parametrization of a force field around the metal from ab initio calculations could provide accurate results, even more than those presented here. However, one should take into account that such a parametrization would involve a computational cost substantially higher than that of IMOMM: here there is only one calculation, with only the standard values of the force field (in this case MM3) being used.

Quantification of "Steric" Effects

The previous section has shown how IMOMM calculations on the real systems **1** and **2** can improve the geometrical description of the system with respect to the results obtained in the ab initio calculation on the model system **3**. This section will go one step further and analyze what are the reasons for such improvement in terms of which of the interactions introduced by IMOMM are the main ones responsible for the geometrical distortion. In other words, this section will analyze which are the main steric effects, understanding by such the interactions neglected in the ab initio calculation on the model system and introduced in the IMOMM calculation of the real system.

In order to do that, a simple computational scheme consisting of several steps is defined: (1) separation of the geometrical variables of the model system in two sets (A, consisting of the geometrical variables which are to be analyzed, and B, consisting of the other geometrical variables); (2) full IMOMM geometry optimization on the real system; (3) full MO optimization on the model system; (4) restricted IMOMM optimization on the real system with the geometrical variables of set A frozen at the values of the MO optimization in the model system; (5) comparison of the results of steps 2 (full IMOMM optimization) and 4 (restricted IMOMM optimization). This scheme will hopefully be clarified through its application to the particular case under study, but some comments are pertinent before entering the discussion of its application. The first of them is that the restricted IMOMM optimization yields the geometry that the system would take should steric effects be absent. Therefore, it is the adequate starting point for comparison with the full IMOMM that is precisely the geometry the system takes after the steric effects are introduced. The second point to remark here is the need for an initial separation of the geometrical variables in step 1. This process allows one to put aside geometrical variables that are deemed unimportant by chemical common sense, but that could influence heavily the analysis. A typical example would be ligand rotation around M−P bonds.

The scheme is applied to both complexes **1** and **2**. Set A is chosen to include the coordinates defining the position of the metal and all atoms directly attached to it. Re−P−C angles and C−P−Re−H(2) dihedral angles have been therefore optimized even in the restricted IMOMM optimization. Completion of the scheme presented above requires only two additional calculations, one for each case, those of the restricted IMOMM optimizations. The other two calculations, full IMOMM optimization and full MO optimization of the model system, have been presented in the previous section.

The first interesting result is obtained from the analysis of the total energies of the restricted and full IMOMM optimizations. The restricted calculation has in all cases a higher energy, as should indeed be expected. But the values are different in both complexes, the difference between full and restricted optimization is 4.9 kcal/mol in the case of **1** and 7.3 kcal/mol in the case of **2**. That is, steric effects are significantly larger in **2**. Or, to be more precise, the energetic cost of the geometrical distortion associated to the introduction of steric effects is significantly larger in **2**. This result has a certain chemical value, and there was no obvious way to predict it a priori. The comparison between the steric repulsions of two PPh^iPr_2 and two $SiHPh_2$ groups on one hand (complex **1**) and two $PCyp_3$ and two SiH_2Ph groups on the other hand (complex **2**) is certainly not straightforward. IMOMM provides in a simple way such a comparison, with the clear diagnostic of a quite more expensive distortion in **2**, as far as the energy is concerned.

The analysis does not have to stop at the total energies. The 4.9 kcal/mol associated with the steric relaxation of **1** can be decomposed in an MM stabilization of 5.3 kcal/mol and an MO destabilization of 0.4 kcal/mol. The numbers for **2** are 10.8 and 3.5 kcal/mol, respectively. While **1** has practically the same MO energy, **2** is destabilized by 3.5 kcal/mol, a new confirmation of the importance of the distortion in **2**. Decomposition of ab initio energies in different terms can be attempted, and there is indeed a wealth of publications on the subject.[22] However, it is obviously much simpler to decompose the molecular mechanics energies as a sum. The results of such a decomposition are presented in the following paragraphs for

(22) (a) Kitaura, K.; Morokuma, K. *Int. J. Quantum Chem.* **1976**, *10*, 325. (b) Morokuma, K. *Acc. Chem. Res.* **1977**, *10*, 294. (c) Kitaura, K.; Sakaki, S.; Morokuma, K. *Inorg. Chem.* **1981**, *20*, 2292.

Table 4. Decomposition of the Molecular Mechanics Part of the IMOMM Energy (kcal/mol) of Complex $[ReH_5(PCyp_3)_2(SiH_2Ph)_2]$ (**2**) in the Complete and Restricted Geometry Optimizations

	complete	restricted	difference
compression	4.72	5.01	0.29
bending	37.33	40.26	2.93
bend−bend	1.60	1.74	0.14
stretch−bend	−1.84	−1.86	−0.02
VdW 1,4	39.75	39.84	0.09
YdW other	−8.18	−0.42	7.76
torsional	31.74	31.42	−0.32
torsion−stretch	−2.06	−2.05	−0.01
dipole−dipole	11.51	11.45	0.06
total	114.58	125.40	10.82

complex **2**, the species found to have a more significant distortion.

Table 4 presents the decomposition of the total MM energy in different terms for the full IMOMM optimization and the restricted IMOMM optimizations of complex **2**, as well as the differences in each of the terms. The total difference of 10.82 kcal/mol comes from two clearly dominating contributions, 7.76 kcal/mol from "VdW other" and 2.93 kcal/mol from "bending". Changes in the other terms are smaller, with the following in absolute value being the 0.32 kcal/mol of the "torsional" term. Therefore, MM effects on this complex can be analyzed essentially in terms of the van der Waals interactions ("VdW other" stands for van der Waals interactions different from 1, 4), with a smaller but nonneglectable contribution of the bending interactions. At this point, it is necessary to remember that the MM force field applied is MM3. This result is very likely affected in a heavy way by the choice of this force field. Other force fields grant a lesser importance to van der Waals terms and give more weight to electrostatic contributions, for instance.[17,23] If such other force fields had been applied, the decomposition presented in Table 4 would likely be substantially different. But, the total difference would have to be similar, because it has been demonstrated in the previous section that the introduction of MM3 contributions through IMOMM improves substantially the quality of the MP2 results. In other words, Table 4 has to be interpreted in the sense that the more significant MM contributions correspond to what MM3 calls van der Waals and bending contributions, without entering in the real chemical meaning of such terms.

Whatever is the real meaning of the van der Waals term, it can be further decomposed in each of the single interatomic repulsions that contribute to it. Because of the difficulty of dealing with the total 6693 interactions, a filter has been used to choose only the most important of them. This consists of taking only the interactions that differ by more than a certain threshold between the two IMOMM calculations. When this threshold is chosen to be 0.05 kcal/mol, only 58 interactions remain, yet they add up to 7.03 kcal/mol, which is a sizable proportion of the total 7.76 kcal/mol of the "VdW other" term. Finally, these 58 interactions have been grouped by the ligand to which each of the two atoms belong, with the results presented in Table 5. The more important contributions are the 2.28 and 2.30 kcal/mol associated with the P(7)−Si(9) and P(8)−Si(10) ligand pairs, which are related by symmetry. They are trailed at a distance by the P(7)−P(7) and P(8)−P(8) pairs, corresponding to intraligand reorganization, with a weight of 0.61 kcal/mol. All other pairs of ligands have a contribution smaller than 0.50 kcal/mol. It can be noticed that the P(8)−Si(9) and P(7)−Si(10) pairs have negative contributions of −0.11 kcal/mol. This simply states the fact that repulsion between these particular pairs of ligands is higher in the fully optimized geometry than in the restricted one. The main conclusion from Table 5 is therefore that the steric stabilization of complex **2** is essentially associated with the relaxation of steric repulsions between P(7)−Si(9) and P(8)−Si(10), with the consequent rearrangement within the P(7) and P(8) ligands.

Table 5. Grouping by Ligand of the Interatomic van der Waals Interactions Changing by More Than 0.05 kcal/mol between the Complete and Restricted IMOMM Geometry Optimizations of Complex $[ReH_5(PCyp_3)_2(SiH_2Ph)_2]$ (**2**)[a]

	Re(1)	H(2)−H(6)	P(7)	P(8)	Si(9)	Si(10)
Re(1)	0.00					
H(2)−H(6)	0.00	0.00				
P(7)	0.24	0.43	0.61			
P(8)	0.24	0.43	0.11	0.61		
Si(9)	0.00	0.00	2.28	−0.11	0.00	
Si(10)	0.00	0.00	−0.11	2.30	0.00	0.00

[a] Contributions from the hydride ligands H(2) to H(6) are grouped in a single term.

The conclusions of the previous paragraph are further confirmed when a similar analysis is carried out on the "bending" term. With the same threshold of 0.05 kcal/mol, 32 out of 270 interactions have to be considered, representing 2.36 out of the total 2.93 kcal/mol of the "bending" term. All of these 32 bending interactions are within the P(7) and P(8) phosphine ligands.

A similar analysis could be presented for complex **1**. It is not reported here because it is obscured by the fact that the C_2 symmetry breaks down in the restricted IMOMM optimization and because the main purpose of the paper is not to discuss the particular features of these complexes but to show the abilities of the IMOMM method. Finally, we would like to mention that the type of analysis that has been just presented is not the only one that can be derived from the scheme presented in this section. For instance, the study of the steric interactions on one particular hydrogen atom of the ligands could allow the prediction of the sensitivity of the total geometry to its substitution by a bulkier ligand.

Conclusions

The geometry optimization at the IMOMM(MP2:MM3) level of the $[ReH_5(PPh^iPr_2)_2(SiHPh_2)_2]$ and $[ReH_5(PCyp_3)_2(SiH_2Ph)_2]$ complexes yields results that are significantly more similar to X-ray and neutron diffraction structures than those of the MP2 optimization of the model system $[ReH_5(PH_3)_2(SiH_3)_2]$, and this is done with a very similar computational cost. A simple computational scheme has been defined that permits a further analysis of the steric effects through IMOMM. It allows the energetic quantification of the distortion associated with the steric effects, which is shown to be larger in $[ReH_5(PCyp_3)_2(SiH_2Ph)_2]$ than in $[ReH_5(PPh^iPr_2)_2(SiHPh_2)_2]$. Finally, IMOMM can also indicate the main contributions to steric relaxation. In the case of $[ReH_5(PCyp_3)_2(SiH_2Ph)_2]$ they are shown to be the repulsions between the P(7)−Si(9) and P(8)−Si(10) pairs of ligands.

Acknowledgment. Financial support is acknowledged from the Spanish "Dirección General de Investigación Científica y Técnica" (DGICYT) under Projects No. PB92-0621 and PB95-0639. Y.J. acknowledges partial support by the Human Capital and Mobility Programme, Access to Large Installations, under Contract CHGE-CT92-0009, "Access to supercomputing facilities for european researchers" established between The European Community and CESCA/CEPBA. Support is also acknowledged from the "Acción Integrada Hispano-Francesa" Grant No. 228B.

IC960440K

(23) (a) Brooks, R.; Bruccoleri, R. E.; Olafson, B. D.; States, D. J.; Swaminathan, S.; Karplus, M. *J. Comput. Chem.* **1983**, *4*, 187. (b) Weiner, S. J.; Kollman, P. A.; Nguyen, D. T.; Casey, D. A. *J. Comput. Chem.* **1986**, *7*, 230.